Vol. 44, No. 4 (2022) 568-583, DOI: 10.24874/ti.1315.06.22.09

Tribology in Industry

www.tribology.rs

RESEARCH

Wear Characteristic of ZrO_2/MGO as Lubricant in Different Rotating Speed

Dharmender Singh Saini[a,*] and Surendra Pal Singh Matharu[a]

[a]*Department of Mechanical Engineering, NIT Raipur, Chhattisgarh, INDIA- 492010.*

Keywords:

Tribology
Zirconia
Nanofluid
DOE
Taguchi

* Corresponding author:

Dharmender Singh Saini
E-mail: dharmender.saini13@gmail.com

Received: 7 June 2022
Revised: 3 August 2022
Accepted: 13 September 2022

A B S T R A C T

Proper rolling bearing lubricants and lubrication procedures are critical for delivering adequate bearing performance in critical situations. Main roles of Zirconium di oxide (ZrO_2) nanoparticles in engine oil as lubricant additive for rolling bearing are reduction of wear and friction, extension of fatigue life, removal of frictional heat, and protection from corrosion. The present work investigates the tribological properties of SAE20W40 MGO and ZrO_2 nano particles in SAE20W40 MGO oil for 0.4% concentration between steel/steel contact. In order to study wear under variable speed conditions, four-ball wear tests were carried out with chrome-plated steel balls (Grade E-52100), which were designed using 2 levels of factorial design of experiments (DOE). Nano-lubricant deterioration with and without ZrO_2 were determined using empirical equations to project wear with reference to speed and ZrO_2 concentration. Results presented that anti-wear properties of the SAE oil samples enhanced with ZrO_2 irrespective of speed range.

© 2022 Published by Faculty of Engineering

1. INTRODUCTION

The search of energy saving and failure reduction in industry sectors is never-ending. Friction loses a lot of energy, and wear diminishes the equipment's life and causes catastrophic breakdowns. Improving the efficiency of the lubricating medium is a common way for lowering the coefficient of friction and increasing wear resistance in order to increase the efficiency of industrial production. Lubricants, such as oil or grease, can help to reduce wear and friction in mechanical components. The wear on the contact surface is significant in particular cases, such as the mesh of gear pairs, the start-up of mechanical assembly, and the direction change of the engine piston [1]. Conventional lubes are unable to satisfy the needs of modern industry, as evidenced by their poor performance in anti-wear, anti-corrosion, extreme pressure, and frictional reduction capabilities [2]. To overcome this, there has been a growing trend of dispersing various types of nanoparticles in base fluid to increase their anti-wear, extreme pressure, anti-corrosion, frictional reduction and thermal performance [3–5].

Nanoparticle dispersion modifies the coefficient of friction and anti-wear characteristics of the base fluid. As previous study stated that, the

lubricant mechanism with nanoparticles includes surface polishing action, rolling, patching, mending, and tribo-film production [6–10]. According to Tao et al. [6] the rubbing surfaces are penetrated by diamond nanoparticles mixed in paraffin oil and operate as a ball bearing, converting sliding action into rolling motion. Using scanning tunnelling microscopy, Liu et al. [8] detected the mending effect in wear scar due to the deposition of Cu nanoparticles. Zhou et al. [9] discovered that the Cu nanoparticles interact with the friction surfaces to generate a tribo-film, that improves the friction surfaces anti-wear performance. Tang et al. [10] discovered that the surface polishing action reduces surface roughness, resulting in micro-plateaus with highly polished surfaces and approximately constant height. Kaviyarasu and Vasanthan [11] reported 54% decrease in coefficient of friction for 20W40 engine lubricant by 0.1% volume fraction of Cu nanoparticles of APS 40nm. Ali et al. [12] reported 40-51% decreases in friction loss and 17% decreases in wear rate for SAE 5W30 lube oil using 0.05% of hybrid (Al_2O_3/TiO_2) nanoparticle APS of 10nm. Padgurskas et al. [13] used Cu, Fe and Co nanoparticle of APS of 50-80nm in SAE 10 engine lubricant and found that at 0.25% volume fraction this prepared nano-lubricant shows 47%, 23% and 11% reduction in wear. Battez et al. [14] reported reduction in friction and wear for POA 6 of CuO, ZrO_2 and ZnO nanoparticles. Bhaumik et al. [15] used castor oil with ZnO nanoparticle at 0.1% optimum volume fraction found that friction and wear is minimum compare to base lubricant. Several study has been performed to characterize nano-lubricant for wear and friction [16–20].

Nanoparticles not only influence the tribological properties of mineral oil, but also have a very good influence on grease and bio-based lubricants. Grease is a semi-solid lubricant made up of base oil (mineral/bio-lubricant), thickeners, and, if desired, other additives to improve the properties of grease. 1% wt. fraction of TiO_2 nanoparticle distributed in lithium grease, Chang at el. [21] found approx. 40% reduction in friction coefficient, and 2% wt. fraction of CuO nanoparticles in lithium grease showed the best anti-wear performance which reduced the wear to 60%. Mohamed et al. [22] added 1% weight fraction of CNTs to lithium grease which greatly increased anti-wear performance (reduce WSD by roughly 63%), decreased friction coefficient (reduce CoF about 81.5%) and increased extreme pressure (EP) properties up to 52% at 1% weight fraction of CNT in lithium grease. He et al. [23] reported that SiO_2 nanoparticles with an APS of less than 100 nm were added into the lithium grease at a weight fraction of 0.3%. SiO_2-nanogrease showed the lowest COF and WSD. Several studies were performed to study anti-wear and friction performance with TiO_2, ZrO_2, Calcium borate, CNT, MWCNT, MWCNT/Talc powder, CaF_2, CeF_3 nanoparticle in lithium and calcium base grease were studied by researchers [24–29]. Despite the fact that many researchers have worked hard to explore the tribological features of ZrO_2 as additions. The majority of them were primarily concerned with investigating the friction-reduction and anti-wear properties of ZrO_2 as lubricant additives (PAO 6, Avocado oil, 20# machine oil, and so on) [14,30–32] or grease additive [27,33,34]. However, it is commonly accepted in mechanical engineering that the performance deterioration or even failure of mechanical equipment occurs in service life and surface quality of components, which arise from the point contact of friction pairs under different operating speed. It needs to be seen if ZrO_2 can perform its function at point contact under varied motion modes. As a result, further tests are required to get a thorough conclusion. ZrO_2 is employed as an oil additive in this research to investigate its tribological performance in friction and wear reduction for AISI E52100 chrome coated steel balls moving against three stationary balls under various operating speeds. As part of the DOE matrix, 8 different test conditions were studied, with triplicates for each condition. We calculated each WSD from each of the three clamped balls for each test, and then used DOE to calculate and analyse the mean, followed by presenting the comparison. The four-ball machine's friction coefficient figures were presented. Inverted Metallurgy Microscopy was used to assess the wear surface.

Nano-lubricant wear mechanisms at different speeds were compared to those of base fluid. Using a multigrade engine lubricant, this research examines ZrO_2 wear behaviour under varying speed conditions to simulate actual application conditions as opposed to testing it according to ASTM standards wherein all other parameters are held constant except for speed.

2. MATERIAL PREPARATION AND EXPERIMENTAL DETAIL

2.1 Characterization of nanoparticles

Zirconium di-oxide (ZrO_2) also known as Zirconia. It's a white zirconium crystalline oxide. The mineral baddeleyite has a monoclinic crystalline structure, which is its most common natural form [35,36]. Zirconia is made by calcining zirconium compounds and taking advantage of their great thermostability [37]. ZrO_2 nanoparticles having excellent properties like chemical stability, crystallinity, corrosion resistance and hardness [32]. In the present work, ZrO2 (d_p=20nm) nanoparticles procured from Nanoshel Ltd (India). Nanoparticles dry in a hot air oven at 100 °C for 1 hour to remove moisture. After that, the obtained nanoparticle was ultrasonicated so that if there is any agglomeration, it can be removed. Then the obtained nanoparticle was put in an airtight container and taken for a FESEM. Further, Field emission scanning electron microscopy (Carl Zeiss UHR FESEM Model Gemini SEM 500 KMAT) was used to validate the shape and size of procured particles from supplier it was found that the average particle size was d_p=31.60nm. The working distance of the FESEM was 8.1mm and the voltage was 3.00 kV. Fig. 1 (a) shows the FESEM image of procured sample, and Fig. 1 (b) show the size distribution of nanoparticles. Further, Energy Dispersive X-ray (EDX) results shown in Fig. 1 (c). The peak of Zr and O (oxygen) confirm the elemental composition of ZrO_2 (Zirconium di-oxide). This study does not provide a precise sample quantification; but, based on the peaks, it may be concluded that Zr and O are present in greater proportions. The physical properties of ZrO_2 nanoparticles are listed inTable 1.

Table 1. Properties of ZrO_2 nanoparticles (CAS: 1314-23-4).

Nano Powder	Property
Zirconium dioxide (ZrO_2)	Appearance - White, Purity - 99.9%
APS as per supplier	20 nm
APS as per FE-SEM	31.60 nm
Molecular formula	ZrO_2
Molecular weight	123.218 g/mol
Density	5.68 g/cm^3
Thermal conductivity	≈2.2 W/m.K

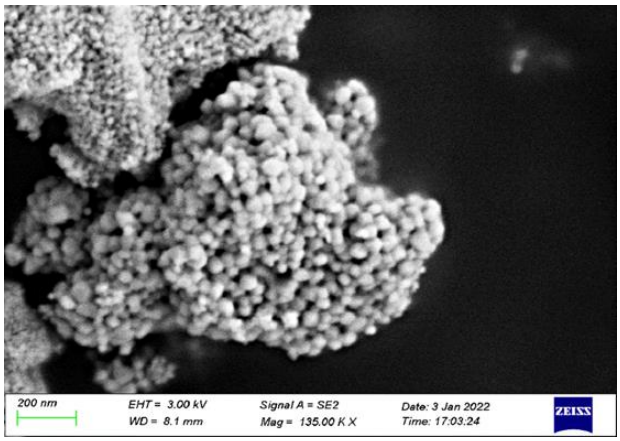

(a)

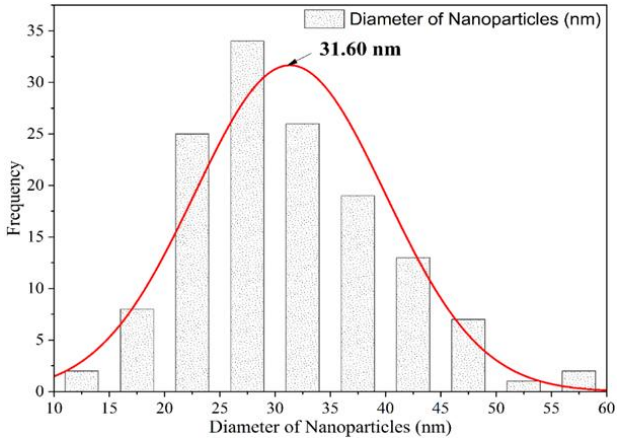

(b)

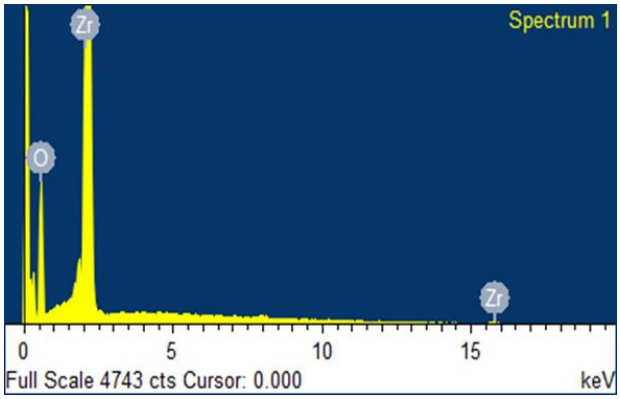

(c)

Element	Weight %	Atomic %
O K	33.79	74.42
Zr L	66.21	25.58
Totals	100.00	

Fig. 1. (a) FESEM image at 135K X resolution (b) particle size distribution, and (c) EDX analysis.

2.2 Preparation of nano-lubricant

Castrol SAE_20W40 multigrade engine oil (MGO) purchased from local market were selected as the base oil for the preparation of nano-lubricant for tribological tests. Lubricants used nowadays having

a variety of additives such as corrosion and rust inhibitors, antioxidants, and anti-wear compounds [38]. In this research, no additive dispersant (surfactant) was mixed to the base fluid. Table 2 show the properties of base fluid used for this study. Nano-lubricants are made in two steps, with nanoparticles added to the lubricant separately by magnetic stirring. Additionally, ultrasonication results in the homogeneous mixing of nanoparticles in oil. An electronic weighing equipment was used to measure the mass of the required volume fraction having least count of 0.001mg. Nanoparticles with a volume fraction of 0.4 percent are introduced to the base fluid. Fourier transform infrared spectroscopy (FTIR) and visual sedimentation test (Fig. 3) of the nano-lubricant show that the nanoparticles are stable after magnetic stirring and ultrasonication, and the experiments are performed shortly after ultrasonication for better results. Volume fractions for tribology testing are obtained using Eq. (1).

$$Volume\ fraction\ (\emptyset) = \frac{\frac{w_{np}}{\rho_{np}}}{\frac{w_{np}}{\rho_{np}} + \frac{w_{bf}}{\rho_{bf}}} \quad (1)$$

Where, $\emptyset$ is the volume fraction of ZrO_2 nanoparticles in SAE_20W40 multigrade engine lubricant, w_{np} is weight of nanoparticle, w_{bf} is the weight of MGO, ρ_{np} is the density of nanoparticles and ρ_{bf} is the density of MGO respectively.

Table 2. Specifications of SAE 20W40 engine oil.

Specification	Value
Density	0.882 g/ml
Viscosity at 40°C	122.80 mm²/s
Viscosity at 100°C	14.0 cm²/s
Viscosity Index	110
Thermal Conductivity	0.135 W/m.K

2.3 Experimental details

In line with ASTM D4172, the Four-ball wear tester (Model: Ducom Instruments Pvt. Ltd., Make: TR-30H-IMTR) has been widely applied to analyze the wear performance of metal-metal contact in the presence of lubrication. Except for the speed, which was adjusted from 600–1500 rpm at an interval of 300 and the other test constraints in this study were governed by the ASTM D4172 standard [39]. The balls were made of AISI E-52100 (12.7 mm in diameter; hardness: 60-66 HRc).

Table 3 ASTM test parameters and test materials properties for four-ball tester.

Test Parameter	
Applied Load (N)	392 ± 5
Fluid Temperature (°C)	75 ± 1
Test duration (s)	3600 ± 10
Speed (RPM)	(600, 900, 1200, 1500) ± 10
Test Material	
Ball materials	AISI E52100 (Chrome alloy steel balls)
Composition	1.3 ≤ Cr ≥ 1.6, 0.96 ≤ C ≥ 1.11, 0.24 ≤ Mn ≤ 0.44, Fe: - balance
Diameter of Balls (mm)	12.7
Hardness (HRc)	60-66

Table 3 gives the ASTM test parameters and test material characteristics, except for speed. The ASTM standard employs defined experimental settings to correctly conduct a testing methodology that involves heating the lubricant to 75°C before applying load. For heating lubricant the four ball wear tester is equipped with heating cartridge which is located at the bottom of ball pot assembly as shown in figure 1c. And thermocouple keeps the check on temperature of lubricant for maintaining lubricant at constant desired temperature. Lubricant service life is greatly reduced at temperatures above 60 °C and at high speeds, hence vehicle engine service life is highly dependent on lubricant service life.

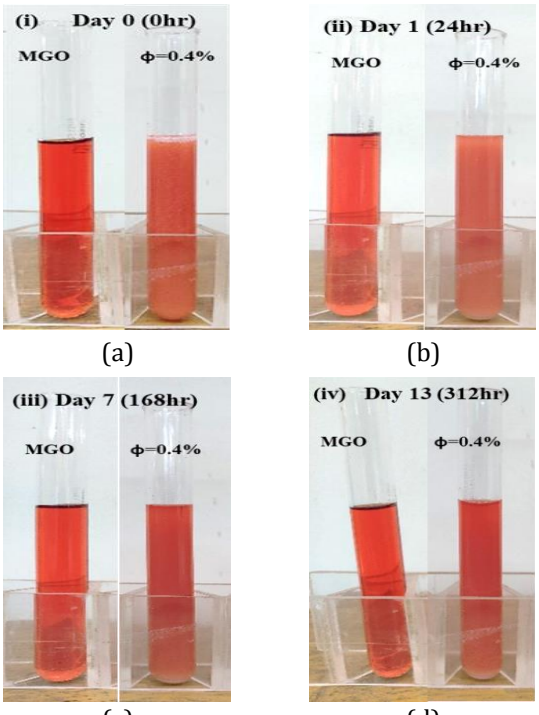

Fig. 2. Photograph of MGO and ZrO_2/MGO sample at different interval of time.

Fig. 3 (c) shows a schematic diagram of a four-ball wear machine. Three lower balls were positioned in a steel cup in a fixed position (shown in Fig. 3 (a)), while the others were retained in the top chuck (shown in Fig. 3 (b), which rotated. The steel cup was filled with plenty of test fuel (about 10 ml) to cover the lowest three balls to a depth of at least 3 mm (shown in Fig. 3 (c)).

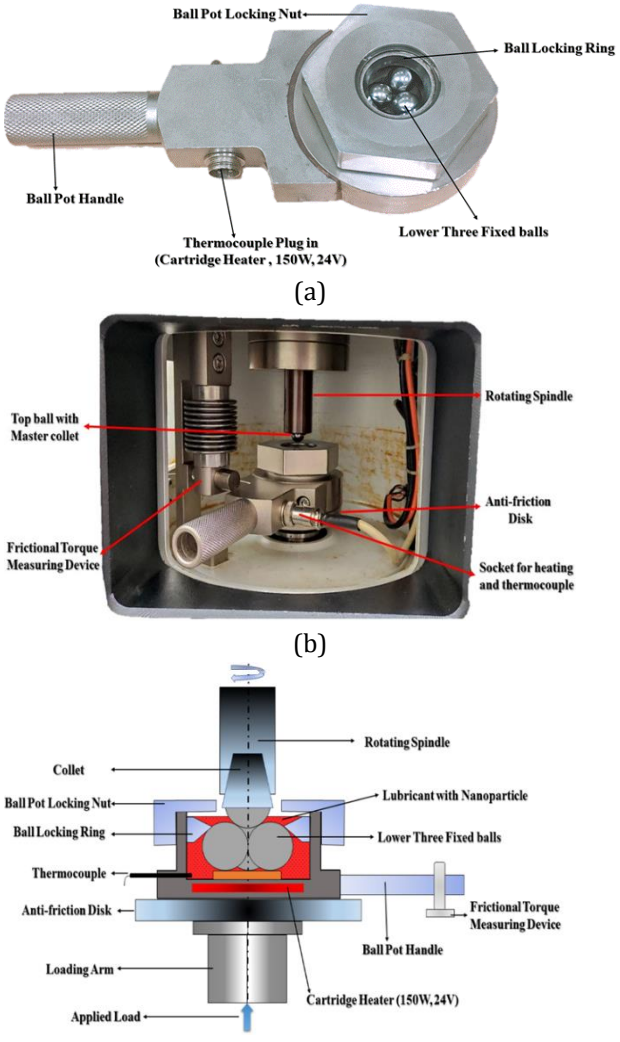

Fig. 3. (a) Lower three ball in ball pot assembly, (b), (c) Schematic diagram of four ball tester.

To record the friction torque, the Four-ball wear tester was connected with wired to a computer. The friction torque of test was converted into friction coefficient by eq. (2). The tests were repeated three times, with the average value of the readings given. An optical microscope was used to measure the wear scar diameters of the steel balls before they were removed from the cup. The average wear scar diameter of the lowest three balls is presented here. After that, acetone was used to thoroughly wash them. An inverted optical microscope was then used to examine the worn surfaces of the balls (Model: BX3M-LEDR, Make: Olympus).

$$Coeffecient\ of\ Friction\ (\mu) = \frac{T.\sqrt{6}}{3.W.r} \qquad (2)$$

Where, T is the friction torque (N.m), W is the applied load (N), and r is the distance between the lower balls' contact surfaces and the axis of rotation (which is 3.67 mm).

2.4 Design of experiments (DOE)

Taguchi is an extremely powerful method for analysis. The number of experiments is reduced by using orthogonal arrays and the effect of uncontrollable factors is minimized. Further, it provides a simple, efficient and systematic way to identify the best parameter on a tribological test [40,41].

Using the Taguchi method, the difference between experimental and desired values is calculated using a loss function. Further, the loss function is converted to the signal-to-noise ratio (S/N) [42,43]. Normally, S/N ratios are analyzed according to three kinds of quality characteristics: lower is better, higher is better, and nominal is better [41]. S/N ratios are determined based on the S/N analysis for each of the process parameters. This study aimed to minimize the CoF and WSD. eq. (3) shows that the smaller-is-better quality characteristic is applied in this study.

$$S/N_s = -10 * \log_{10}\left(\frac{\sum_{i=1}^{n} Y_i^2}{n}\right), \quad lower-the-better\ (Minimum) \qquad (3)$$

Where, the observed values at the i^{th} experiment are y_i, and the number of observations is n.

Speed, and volume fraction of nanoparticles in raw oil were selected as control factor and their level were determine as shown in Table 4. To identify the best tribological parameters and investigate the impacts of parameter [44], the most suitable complete factorial design with orthogonal array L_8 (4^1 x 2^4) was chosen. The trials were carried out using the L_8 mixed orthogonal array given in Table 5.

Table 4 Tribological parameters and their levels.

Parameters	Symbol	Level 1	Level 2	Level 3	Level 4
Speed (RPM)	A	600	900	1200	1500
Volume Fraction (%)	B	0	0.4	-	-

Table 5. Full factorial with orthogonal array L8 (4^1 x 2^1).

Experiment number	Factor A	Factor B
1	600	0.0
2	600	0.4
3	900	0.0
4	900	0.4
5	1200	0.0
6	1200	0.4
7	1500	0.0
8	1500	0.4

3. RESULTS AND DISCUSSION

3.1 Nanoparticle size and morphology

Fig. 1, shows the size, morphology, and variation of the ZrO_2 nanoparticles. The nanoparticles' shape appears to be spherical in nature, this was similar to the manufacturer's specification. The sizes of 136 particles were determined using IMAGE-J software (particle distribution shown in Fig. 1 (b)). It was determined that the size of ZrO_2 particles was 31.60nm. This was larger than the manufacturer's specification. It is possible that the agglomeration of nanoparticles caused this increment.

3.2 Dispersion stability

The stability of nano-lubricant is very important. After the preparation of nano-lubricant, it is always recommended to do its stability analysis. Visualization method, UV–Vis Spectro-photometer, DLS, zeta potential, Imaging method (optical microscope, SEM, TEM, FESEM) analysis are common method to check the stability of nano-lubricant [45]. FTIR test is commonly used to determine chemical composition of nano-lubricants. Fig. 4 show the FTIR spectra for pure SAE_20W40 oil (MGO), as well as for 20nm ZrO_2/MGO nano-lubricant. Both the plain and nano-lubricant samples have nearly identical FTIR spectra, with no new peaks apparent. In both cases, the FTIR spectrum shows no signs of chemical interaction between nanoparticles and base lubricants. FTIR analysis of Plain MGO and ZrO_2/MGO across a spectral range of (4000–500 cm−1) in the absorbance mode is shown in Fig. 4. The FTIR spectrum for Plain Mineral oil exhibits the C–H symmetric stretching vibration (2920, 2851 cm−1), CH_2 in-plane bending (1455 cm−1), C–C stretching (1377 cm−1) [46,47]. As a result, nanolubricant are chemically stable.

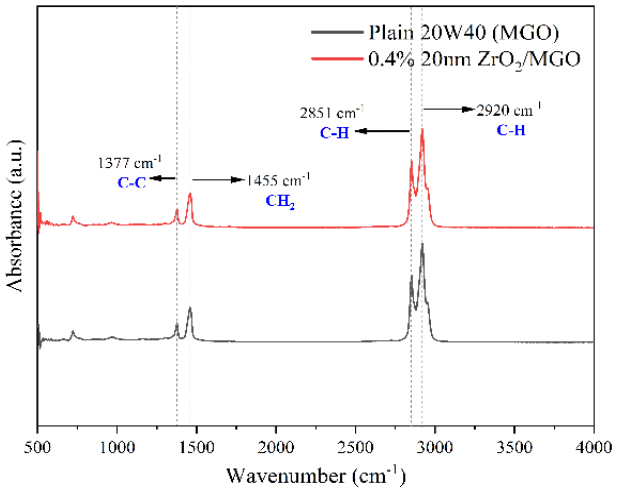

Fig. 4. FTIR spectrum of plain MGO and ZrO_2 of 20nm at 0.4 vol fraction.

3.3 Friction and wear under variable speed

Tests were performed using nano ZrO_2 suspensions at 0.4% volume fraction in 20W40 multigrade oil (MGO). The fourball test machine used at 392N, 75°Cfor one hour at different speeds. WSD of stationary balls was measured after the test after and time, speed, friction torque and test oil temperature were continuously measured during the test run. After the test this friction torque were converted into CoF by Eq.(2).

In Fig. 5, the relationship between CoF and speed for plain MGO and ZrO_2/MGO nano-lubricant compositions can be seen. Both show similar characteristics for the variation in CoF. The anti-friction tests proved that ZrO_2 nanoparticles added to MGO at a concentration of 0.4%, actually reduced friction at the interfaces by an important amount. This was confirmed by repeatability and validity tests under similar conditions. Fig. 5 shows the CoF values for MGO and ZrO_2/MGO obtained during the test at different speeds of the four conditions for both lubricants. At 1500 RPM reduction in coefficient of friction was found to be maximum when compare to lubricant without nanoparticles. At 1200RPM, the minimum reduction was 7.46%, while it reduced the friction coefficient by 9.77% at 1500RPM.

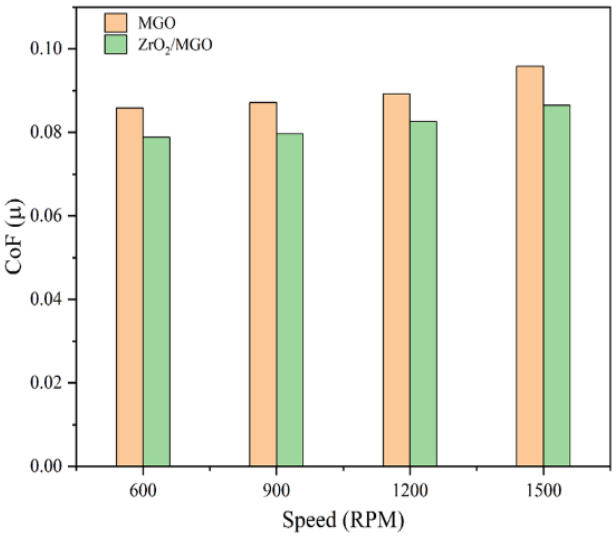

Fig. 5. Coefficient of friction (CoF) of plain lubricant and ZrO_2 nanoparticle mixed lubricant at different speed.

The significant increase in CoF was due to wear caused by moving parts at different speeds. Also, it indicates that an insufficient film was primarily formed on the pairing surface[48]. Throughout the test, the raw oil had a higher CoF value. Due to the generation of metallic debris during sliding, the tribo-film may be continually broken due to the friction generated by the metallic debris [48,49]. Compared to raw oil, the CoF of nano-lubricant was significantly lower at all speeds. Because of the flash temperature created by friction, the nanoparticles absorbed the chemical properties of the metal friction surface via the hydroxyl groups [50,51]. With the stream of lubricant, nanoparticles enter the friction zone. As a result, sliding friction becomes rolling friction [6]. Therefore, both anti-friction effects and ball-bearing effect could be observed. The friction reduction is only better when the nanoparticle concentration is at an optimal level [52].

Additionally, wear scars were measured and analyzed in order to see how speed and nano-particle affected measurable changes in raw oil and nano-lubricant. Wear scars were measured using an optical instrument. The pictures of all of the tests on different operating speeds were taken with an optical microscope and inverted microscope at 20X zoom as shown in Fig. 6 and Fig. 7. The calculated WSD for different operating speeds are shown in Fig. 7. For raw oil, Fig. 6 shows the WSD and surface morphology of worn surface. When the anti-wear test was conducted without any additive, the base oil showed higher material removal, and 495.81 μm of WSD was observed at 1500 RPM. The smooth areas in Fig. 6 (a) indicate a low-wear track with few deep furrows. The material overload and asperity collision resulted in grooves when inspected under higher magnification (Fig. 6 (h)). With raw oil, it is clear that the size of the wear scars increases with increasing in speed. Nanoparticles reduce WSD as they blend into raw oil.

ZrO_2/MGO nano-lubricant wear scars and their surface morphology are shown in Fig. 7. A wear scar is deep and furrowed in Fig. 7 (e-h) as a result of wear and tear relatively than elastic distortion. For all speeds, ZrO_2/MGO nano-lubricant shows smaller wear scars compared to raw oil at 0.4% volume fraction. The following table presents the WSD, WV, and MWV of nanolubricant over a range of speeds: 600, 900, 1200 and 1500 RPM. The Fig. 8 and Fig. 9 depict the comparison of WSD, WV, and MWV of raw and nanolubricant for all lubricants. Based on the experimental results, it is obvious that MGO oil with nano-additives at low speed significantly improves the anti-wear property. When ZrO_2 nano-lubricants are used at a concentration of 0.4% volume fraction at 600RPM, the minimum WSD is 356.42 μm; for additives at 1500RPM it is 476.79μm. For this concentration of 0.4%, these operational speeds were considered optimal. ZrO_2 nano-particle has reduced WSD by a minimum of 1.44 and a maximum of 6.29 % when compared with raw castor oil. A similar wear variation was observed in other concentrations in Table 6.

In other words, particle size affects anti-wear behavior. In the case of WSD increments, it may be related to third body abrasion due to nanoparticles that are deposited between the contacting surfaces after reaching lowest wear [53]. Wäsche et al. [54] reported that nano-additive layers go through a process during which they undergo in-situ micro shearing. During this process, secondary particles of relatively smaller size are produced (secondary nanoparticles or wear debris). They fill the valleys and dimples created by asperity-asperity separation and support the smaller nanoparticles. To maintain load and provide low shear strength at the interface, larger size

particles polish and form a protective layer after polishing the micro-bumps. The tribological performance of nanoparticle-based lubricants has been improved by, (i) Nanoparticles reduce the asperity–asperity contact between the pairing surfaces, thereby reducing real area of interaction, (ii) It prevents/reduces plastic deformation and material removal by acting as a nano-bearing that slides and rolls between pairing surfaces, (iii) Small particles allow the surface to be repaired (mended) by packing in surface valleys and dimples in order to parity surface mass loss, while larger particles form monochrome or multichrome protective films to isolated the pairing surfaces, and (iv) In addition, during the running-in period, surfaces are polished with irregularly shaped hard particles to reducing the surfaces roughness [8,10,49,55–57].

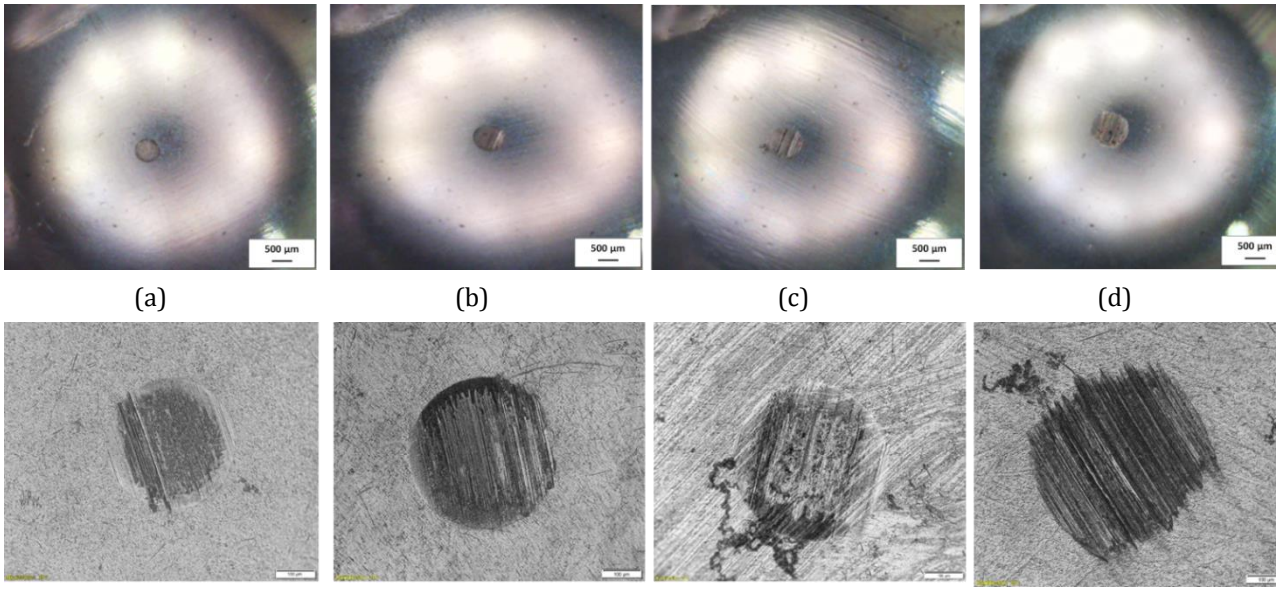

Fig. 6. (a-d) are optical images of Ducom microscope and (e-h) are inverted microscope images at 20x magnification for plain MGO. Where, (a) & (e) at 600RPM, (b) & (f) at 900RPM, (c) & (g) at 1200RPM and (d) & (h) at 1500RPM.

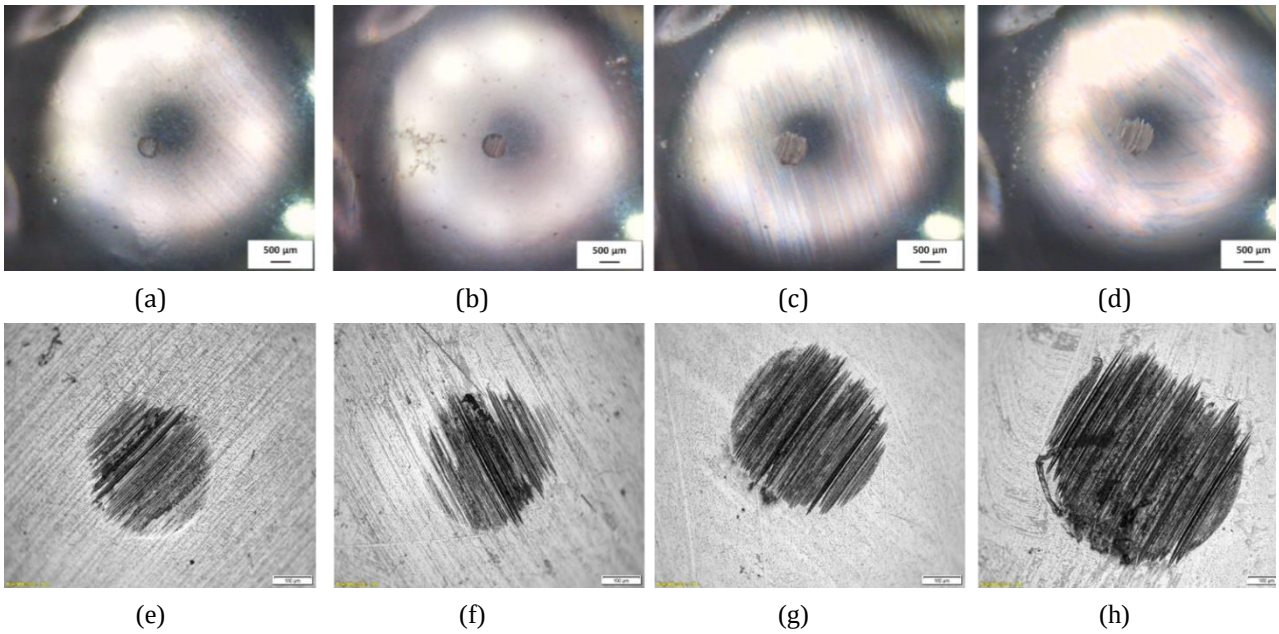

Fig. 7. (a-d) are optical images of Ducom microscope and (e-h) are inverted microscope images at 20x magnification for ZrO_2/MGO. Where, (a) & (e) at 600RPM, (b) & (f) at 900RPM, (c) & (g) at 1200RPM and (d) & (h) at 1500RPM.

Table 6. Variation of WSD. WV and MWV for different operating speed for raw oil and nano lubricant.

Speed (RPM)	Wear scar diameter (µm)	Wear variation (%)	Mean wear volume ($x10^{-4}$ mm^3)	Wear scar diameter (µm)	Wear variation (%)	Mean wear volume ($x10^{-4}$ mm^3)
	Raw Oil (SAE 20W40)			ZrO_2/MGO		
600	361.6317	-	1.14	356.4217	-	1.01
900	389.2233	7.63 ↑	1.93	364.7167	2.33 ↑	1.22
1200	456.67	26.28 ↑	4.82	433.8	21.7 ↑	3.67
1500	495.8056	37.1 ↑	7.28	476.7933	33.77 ↑	6.01

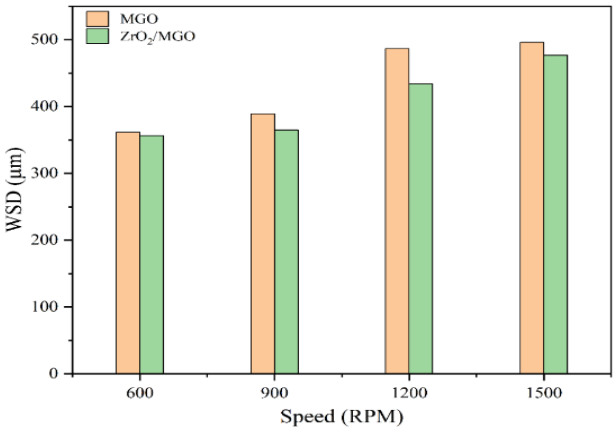

Fig. 8. Variation of WSD for different speed for MGO and ZrO_2/MGO.

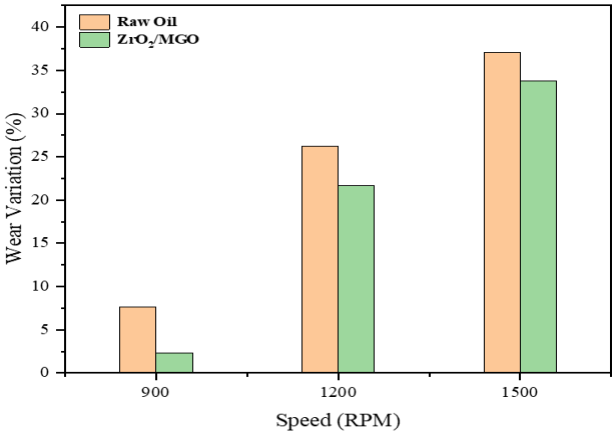

(a)

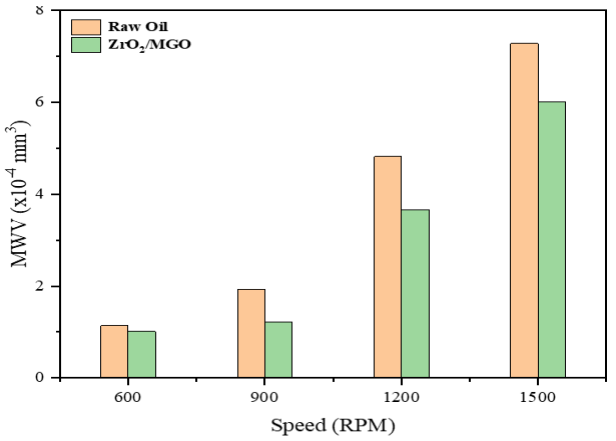

(b)

Fig. 9. Variations in (a) Wear reduction and (b) Mean wear volume (MWV) for different speed.

3.4 Design of experiment analysis

The friction coefficient (CoF) and wear scar diameter (WSD) were measured using Taguchi techniques for every combination of the control factors. Measured control factors were optimized using signal-to-noise ratios (S/N). For a product to be more efficient and improve its tribology, its CoF and WSD should be as low as possible. As a result, the S/N ratio was calculated using the "smaller-is-better" equation. Table 7 shows values for Coefficient of Friction and wear scar diameter in terms of S/N ratios. According to the results of the tests, the average CoF value is 0.086, and the average WSD is 0.41 mm. CoF and WSD have S/N ratios of 21.356 dB and 53.332 dB, respectively.

Table 7. Experimental design and S/N ratio values.

Experiment number	Controlling Factor		S/N ratio for CoF (dB)	S/N ratio for WSD (dB)
	A Speed (RPM)	B Vol. Fraction (%)		
1	600	0.0	21.327	-51.165
2	600	0.4	22.070	-51.039
3	900	0.0	21.197	-51.804
4	900	0.4	21.976	-51.239
5	1200	0.0	20.991	-53.192
6	1200	0.4	21.664	-52.746
7	1500	0.0	20.367	-53.906
8	1500	0.4	21.259	-53.567

In order to evaluate the properties of each of the control factors (Speed and Volume Fraction) on the CoF and wear scar diameter, we used an "S/N response table". S/N tables are shown in Table 8 for CoF and WSD. In this table, that was created by using Taguchi method, we can see the optimal coefficient of friction and diameter of wear scars for an optimal friction coefficient. Table 8 contains the level values of control parameter for CoF and WSD, which are shown in Fig. 10(a & b). These graphs provide an easy way of determining the optimal tribological parameters for minimizing the CoF and WSD.

Table 8. S/N ratio table for CoF and WSD factor.

Levels	Controlling Factor			
	Coefficient of Friction (CoF)		Wear Scar Diameter (WSD)	
	A	B	A	B
Level-1	**21.70**	20.97	**-51.10**	-52.52
Level-2	21.59	**21.74**	-51.52	**-52.15**
Level-3	21.33	-	-52.97	-
Level-4	20.81	-	-53.74	-
Delta (Δ = Max-Min)	0.89	0.77	2.63	0.37
Rank	**1**	**2**	**1**	**2**

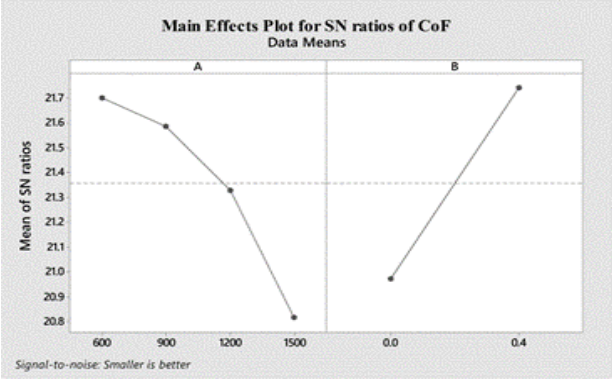

(a)

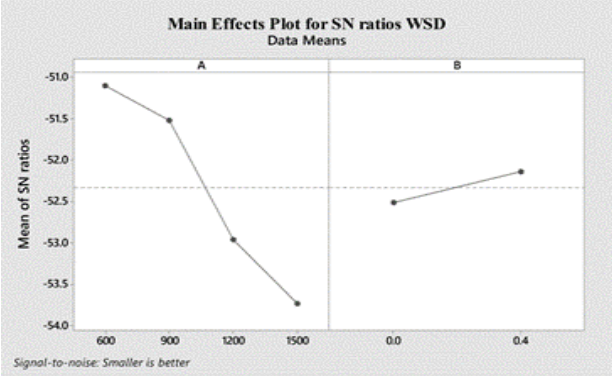

(b)

Fig. 10. S/N ratio of Main Effect plot of (a) CoF and (b) WSD.

A level with the highest S/N ratio was determined for each control factor. Based on these results, the levels and S/N ratios for the factors that gave the best CoF value were as follows: factor A (Level 1, S/N = 21.70), and factor B (Level 2, S/N = 21.74). This means that an optimal COF value could be derived with a 600RPM (A1), and a 0.4% volume fraction (B2) (Fig. 10 (a)). Similarly, best factors given by WSD was at levels and S/N ratios were defined as factor A (Level 1, S/N = -51.10) and factor B (Level 2, S/N = -52.15). According to wear, the optimal WSD value was found to be obtained at 600RPM (A1), and at 0.4% volume fraction (B2) (Fig. 10(b)).

The contour plot of the CoF and WSD model is depicted in Fig. 11 (a&b). Using a Taguchi L8 orthogonal array, we calculated that the friction coefficient decreases as the volume fraction of nanoparticles increases (at 600 RPM) (Fig. 11 (a)). The friction coefficient was significantly reduced by 0.4% nanoparticle in raw oil at high speed (1500 RPM). For 1500 rpm at 0.4% volume fraction of ZrO_2 in raw oil, the minimum friction coefficient was 0.0850. Similarly, a contour map of the WSD is shown in Fig. 11 (b). When raw oil is compared to ZrO_2/MGO oil with 0.4%, wear scar diameter increases rapidly.

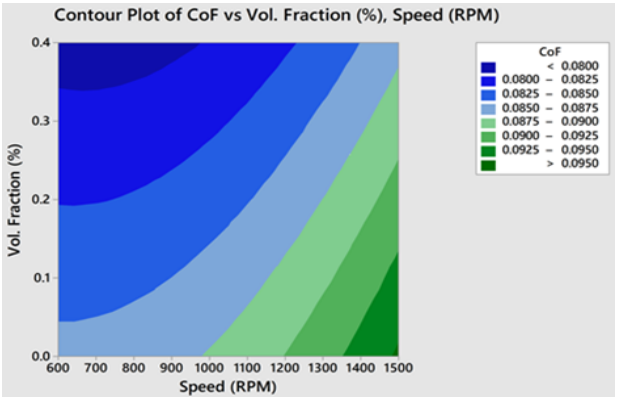

(a)

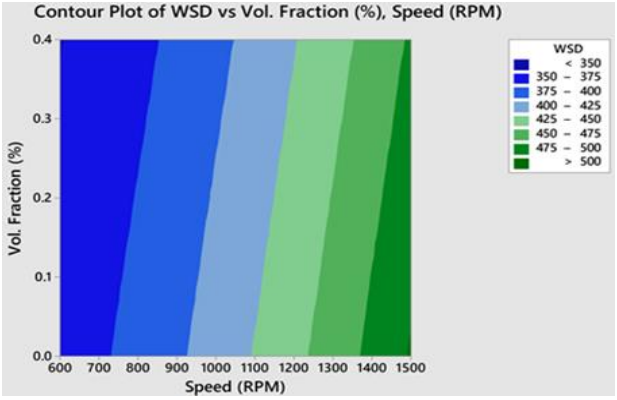

(b)

Fig. 11. Contour plot of CoF and WSD with respect to speed and Vol. fraction (%).

An ANOVA was used to assess the independent or combine effects of all of the different factors in a test. ANOVA analysis was used in order to examine the effect of volume fraction and speed on the CoF and WSD. Table 9 shows the result of an ANOVA for the CoF and WSD. The investigation was conducted at a 95% assurance level and a significant level of 5%. ANOVA determines control factor significance by estimating the F-values of the control factors using Minitab 17. Each parameter's p-value is shown in the last column of the table. According to Table 9, the most important factor affecting the coefficient of

friction and wear was speed (factor A) followed by volume fraction (factor B). After the calculation of significant limitations, the Friction and wear representations were developed by regression equation using only influential coefficients it can be used to do a calculations the CoF and WSD.

Modeling and analyzing several variables involving a dependent variable and one or more independent variables are done using regression analysis [29]. This study used the CoF and WSD as dependent variables, while the speed (V) and volume fraction (Φ) are independent variables. Using regression analysis, we were able to obtain predictive equations for the CoF and WSD. Quadratic regression models were used to make these predictive equations. In eq. (4) and (5), we present the predictive equations of friction coefficient (CoF) and wear scar diameter (WSD):

$$CoF_P = 0.08982 - 0.000014 * V - 0.01369 * \Phi - 5.135E-06 * V * \Phi + 1.169E-08 * V^2 \quad (4)$$

$$WSD_P = 324.9 + 0.022 * V - 9.95 * \Phi - 0.0331 * V * \Phi + 6.4E-05 * V^2 \quad (5)$$

CoF_P and WSD_P present the predictive equations for Coefficient of friction and wear scar diameter. The quadratic regression model predicted the values based on the test results shown in Fig. 12. Based on the figure, it can be seen that the predicted values and the test results are very closely related. Based on the quadratic regression model, the R2 values for CoF and WSD were 99.34% and 96.91%, respectively. Accordingly, the presented regression model was successfully estimating both the CoF and WSD.

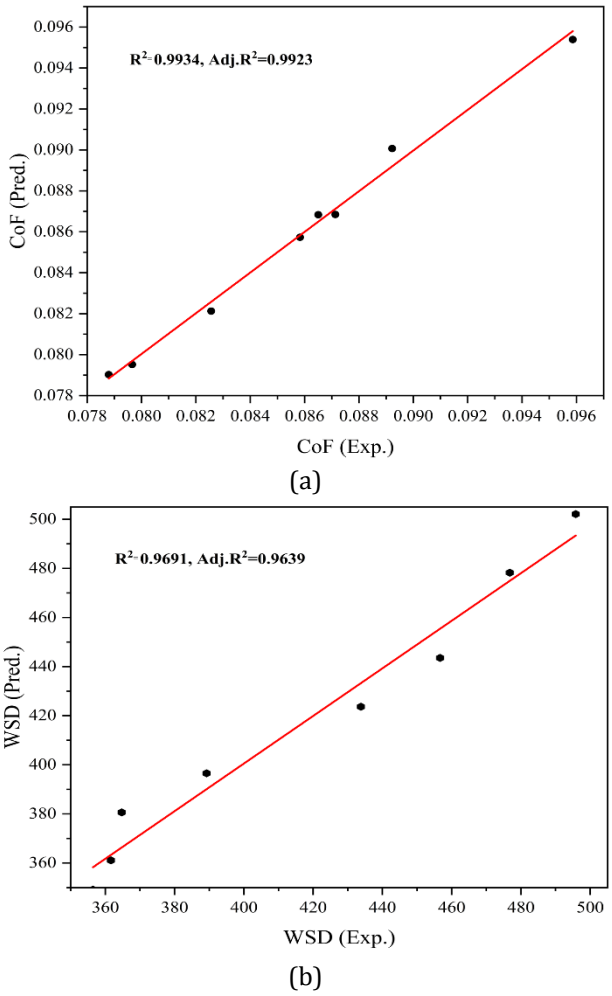

Fig. 12. Comparison of experimental with predicted values of (a) CoF and (b) WSD.

Table 9. ANOVA results of wear scar diameter (WSD) and Coefficient of friction (CoF).

Source	Degree of freedom (DoF)	Sum of Square	Means of Square	F-Value	P-Value
WSD					
Regression	4	21205.1	5301.28	23.50	0.013
Speed	1	6.8	6.75	0.03	0.874
Vol. Fraction	1	2.9	2.93	0.01	0.916
Speed x Vol. fraction	1	39.5	39.54	0.18	0.704
Speed x Speed	1	267.3	267.29	1.18	0.356
Error	3	676.7	225.58		
Total	7	21881.9			
CoF					
Regression	4	2.11E-04	5.30E-05	112.81	0.001
Speed	1	3.00E-06	3.00E-06	5.82	0.095
Vol. Fraction	1	6.00E-06	6.00E-06	11.87	0.041
Speed x Vol. fraction	1	1.00E-06	1.00E-06	2.03	0.250
Speed x Speed	1	9.00E-06	9.00E-06	18.95	0.022
Error	3	1.00E-06	3.333E-07		
Total	7	2.13E-04			

Table 10. Shows the error % between the predicted and experimental measured by Taguchi method and regression equation.

Level	For Taguchi method			For Quadratic regression equation		
	Predicted	Experimental	Error (%)	Predicted	Experimental	Error (%)
CoF (μ)						
A_1B_2 (Optimum)	0.0790	0.0788	0.25 ↑	0.0789	0.0788	0.127 ↑
A_4B_1 (Random)	0.0954	0.0959	0.52 ↓	0.0951	0.0958	0.731 ↓
WSD (μm)						
A_1B_2 (Optimum)	349.183	356.42	2.03 ↓	349.216	356.42	2.021 ↓
A_2B_2 (Random)	380.643	364.72	4.3658 ↑	380.644	364.72	4.3661 ↑

3.5 Validation tests

To verify the control factors for Taguchi method and regression equations at random and optimum levels. A second-order quadratic curve has been used to match the experimental data outputs against the input variables. Using the expression computed using ANOVA, for as φ as concentration and V as speed, as given in Eq. (4 & 5), the friction and wear of nanolubricant are predicted. The results of the suggested mathematical correlation have been validated using the experimental data. Therefore, taking into account R^2 values that are closer to one is important. As shown in Table 10, the comparison between the results of the Taguchi method and those predicted by quadratic regression equations (Eq. (4) &(5)) is shown. These values are very similar to those predicted by the equations. Statistical analyses must have error values below 20% [58]. The error % in the wear are higher than those calculated in the coefficient of friction, both of which are acceptable. As a result, the validation results are valid.

4. CONCLUSIONS

Tribological behavior of a ZrO_2/MGO nano-lubricant was analysied at four different speeds. None of the investigations on the tribological uses of ZrO_2 have been reported; in particular, the inclusion of nano-sized zirconia into lubricating oil with speed variation. All findings were compared to MGO mineral oil without additives. The findings are summarized below:

1. The testing findings revealed that ZrO_2/MGO performed better than raw mineral oil in terms of lowering COF by up to 9.77%.
2. ZrO_2/MGO exhibited great lubricity than raw mineral oil at both lower and higher test speeds, as shown by a low coefficient of friction.
3. In wear scar diameter testing at different testing speeds, ZrO_2/MGO reported lower wear scar diameters at all test speeds. When tested at higher speeds (1200RPM), the ZrO_2/MGO had lower WSD than the raw mineral oil.
4. In terms of WSD, Raw oil showed a larger WSD compared to the ZrO_2/MGO lubricants at higher speed.
5. The WSD, wear variation (WV), and mean wear volume (MWV) of nanolubricant over a range of speeds: 600, 900, 1200 and 1500 RPM was also compared.

In WSD testing at different test speeds, ZrO_2/MGO reported lower WSDs at all test speeds. When tested at higher speeds (1200RPM), the ZrO_2/MGO had lower WSDs than the raw mineral oil:

1. Using S/N ratio, the best amounts of the control parameters for reducing the coefficient of friction and wear were established. The optimum parameters for coefficient of friction and wear were determined at A_1B_2 (i.e., speed = 600 RPM, and volume fraction = 0.4%) and A_1B_2 (i.e., speed = 600 RPM, and volume fraction = 0.4%), respectively.
2. 0.4% volume fraction of ZrO_2 in SAE-20W40 MGO oil exhibited better performance than raw oil.
3. According to data sets, speed was revealed to be the most significant factor for both CoF and wear.

4. The proposed quadratic regression models show a very good relationship between the measured and predicted values for CoF and WSD, with high correlation coefficients (R^2_{CoF}= 0.9934 and R^2_{WSD} = 0.9691).
5. The Confirmation/validation test showed that the measured values were within the 95% confidence region.

In the future, the findings could be applied to academic research as well as automotive and industrial uses. There may be additional factors to be considered in future studies, such as temperature, load, time, and other nanoparticles, all of which affect the coefficient of friction and wear.

REFERENCES

[1] T. Ouyang, Y. Shen, W. Lei, X. Xu, L. Liang, H.S. Waqar, B. Lin, Z.Q. Tian, P.K. Shen, *Reduced friction and wear enabled by arc-discharge method-prepared 3D graphene as oil additive under variable loads and speeds*, Wear, vol. 462-463, 2020, doi: 10.1016/j.wear.2020.203495

[2] T. Ouyang, Y. Shen, R. Yang, L. Liang, H. Liang, B. Lin, Z.Q. Tian, P.K. Shen, *3D hierarchical porous graphene nanosheets as an efficient grease additive to reduce wear and friction under heavy-load conditions*, Tribology International, vol. 144, 2020, doi: 10.1016/j.triboint.2019.106118

[3] S.U.S. Choi, J.A. Eastman, *Enhancing thermal conductivity of fluids with nanoparticles,* Argonne National Lab., IL, United States, 1995.

[4] A. Kotia, P. Rajkhowa, G.S. Rao, S.K. Ghosh, *Thermophysical and tribological properties of nanolubricants: A review,* Heat mass Transfer, vol. 54, iss. 11, pp. 3493–3508, 2018, doi: 10.1007/s00231-018-2351-1

[5] M. Kole, T.K. Dey, *Enhanced thermophysical properties of copper nanoparticles dispersed in gear oil,* Applied Thermal Engineering, vol. 56, iss. 1–2, pp. 45–53, 2013, doi: 10.1016/j.applthermaleng.2013.03.022

[6] X. Tao, Z. Jiazheng, X. Kang, *The ball-bearing effect of diamond nanoparticles as an oil additive,* Journal of Physics D: Applied Physics vol. 29, no. 11, 1996, doi: 10.1088/0022-3727/29/11/029

[7] L. Rapoport, V. Leshchinsky, M. Lvovsky, O. Nepomnyashchy, Y. Volovik, R. Tenne, *Mechanism of friction of fullerenes,* Industrial lubrication and tribology, vol. 54, iss. 4, pp. 171-176, 2002, doi: 10.1108/00368790210431727

[8] G. Liu, X. Li, B. Qin, D. Xing, Y. Guo, R. Fan, *Investigation of the mending effect and mechanism of copper nano-particles on a tribologically stressed surface,* Tribology Letters, vol. 17, iss. 4, pp. 961–966, 2004, doi: 10.1007/s11249-004-8109-6

[9] J. Zhou, J. Yang, Z. Zhang, W. Liu, Q. Xue, *Study on the structure and tribological properties of surface-modified Cu nanoparticles,* Materials Research Bulletin, vol. 34, iss. 9, pp. 1361–1367, 1999, doi: 10.1016/S0025-5408(99)00150-6

[10] Z. Tang and S. Li, *A review of recent developments of friction modifiers for liquid lubricants (2007–present),* Current opinion in solid state and materials science, vol. 18, iss. 3, pp. 119–139, 2014, doi: 10.1016/j.cossms.2014.02.002

[11] T. Kaviyarasu, B. Vasanthan, *Improvement of tribological and thermal properties of engine lubricant by using nano-materials,* Journal of Chemical and Pharmaceutical Sciences, vol. 7, pp. 208–211, 2015.

[12] M.K.A. Ali, H. Xianjun, L. Mai, C. Bicheng, R.F. Turkson, C. Qingping, *Reducing frictional power losses and improving the scuffing resistance in automotive engines using hybrid nanomaterials as nano-lubricant additives,* Wear, vol. 364-365, pp. 270–281, 2016, doi: 10.1016/j.wear.2016.08.005

[13] J. Padgurskas, R. Rukuiza, I. Prosyčevas, R. Kreivaitis, *Tribological properties of lubricant additives of Fe, Cu and Co nanoparticles,* Tribology International, vol. 60, pp. 224–232, 2013, doi: 10.1016/j.triboint.2012.10.024

[14] A.H. Battez, R. González, J.L. Viesca, J.E. Fernández, J.M. Díaz Fernández, A. Machado, R. Chou, J. Riba, *CuO, ZrO2 and ZnO nanoparticles as antiwear additive in oil lubricants,* Wear, vol. 265, iss. 3–4, pp. 422–428, 2008, doi: 10.1016/j.wear.2007.11.013

[15] S. Bhaumik, R. Maggirwar, S. Datta, S.D. Pathak, *Analyses of anti-wear and extreme pressure properties of castor oil with zinc oxide nano friction modifiers,* Applied Surface Science, vol. 449, pp. 277–286, 2018, doi: 10.1016/j.apsusc.2017.12.131

[16] J.L. Viesca, A.H. Battez, R. Gonzalz, R. Chou, J.J. Cabello, *Antiwear properties of carbon-coated copper nanoparticles used as an additive to a polyalphaolefin,* Tribology International, vol. 44, pp. 829–833, 2011, doi: 10.1016/j.triboint.2011.02.006

[17] N. Atiqah, M. Aziz, R. Yunus, U. Rashid, *Temperature effect on tribological properties of polyol ester-based environmentally adapted lubricant,* Tribology Intternational, vol. 93, pp. 43–49, 2016, doi: 10.1016/j.triboint.2015.09.014

[18] X. Song, S. Zheng, J. Zhang, W. Li, Q. Chen, B. Cao, *Synthesis of monodispersed ZnAl 2 O 4 nanoparticles and their tribology properties as lubricant additives,* Materials Research Bulletin, vol. 47, iss. 12, pp. 4305–4310, 2012, doi: 10.1016/j.materresbull.2012.09.013

[19] M. Qu, Y. Yao, J. He, X. Ma, S. Liu, J. Feng, L. Hou, *Tribological performance of functionalized ionic liquid and Cu microparticles as lubricating additives in sun fl ower seed oil,* Tribiology International, vol. 104, pp. 166–174, 2016, doi: 10.1016/j.triboint.2016.08.035

[20] S. Zhang, L. Hu, D. Feng, H. Wang, *Anti-wear and friction-reduction mechanism of Sn and Fe nanoparticles as additives of multialkylated cyclopentanes under vacuum condition,* Vaccum, vol. 87, pp. 75–80, 2013, doi: 10.1016/j.vacuum.2012.07.009

[21] H. Chang, C. Lan, C. Chen, M. Kao, J. Guo, *Anti-Wear and Friction Properties of Nanoparticles as Additives in the Lithium Grease,* International Journal of Precision Engineering And Manufacturing, vol. 15, iss. 10, pp. 2059–2063, 2014, doi: 10.1007/s12541-014-0563-y

[22] A. Mohamed, T.A. Osman, A. Khattab, M. Zaki, *Tribological Behavior of Carbon Nanotubes as an Additive on Lithium Grease,* Journal of Tribology, vol. 137, iss. 1, pp. 1–5, 2015, doi: 10.1115/1.4028225

[23] Q. He, A. Li, Y. Guo, S. Liu, L.H. Kong, *Effect of nanometer silicon dioxide on the frictional behavior of lubricating grease,* Nanomaterials and Nanotechnology, vol. 7, 2017, doi: 10.1177/1847980417725933

[24] L. Wang, B. Wang, X. Wang, W. Liu, *Tribological investigation of CaF2 nanocrystals as grease additives*, Tribology International, vol. 40, iss. 7, pp. 1179–1185, 2007, doi: 10.1016/j.triboint.2006.12.003

[25] G. Zhao, Q. Zhao, W. Li, X. Wang, W. Liu, *Tribological properties of nano-calcium borate as lithium grease additive*, Lubrication Science, vol. 26, iss. 1, pp. 43–53, 2014, doi: 10.1002/ls.1227

[26] L. Wang, M. Zhang, X. Wang, W. Liu, *The preparation of CeF3 nanocluster capped with oleic acid by extraction method and application to lithium grease,* Materials Research Bulletin, vol. 43, iss. 8–9, pp. 2220–2227, 2008, doi: 10.1016/j.materresbull.2007.08.024

[27] M. Wozniak, K. Siczek, P. Kubiak, P. Jozwiak, K. Siczek, *Researches on Tie Rod Ends Lubricated by Grease with TiO2 and ZrO2 Nanoparticles,* Journal of Physics: Conference Series, 2018, vol. 1033, iss. 1, p. 1–911, doi: 10.1088/1742-6596/1033/1/012006

[28] A. Mohamed, S. Ali, T. A. Osman, B. M. Kamel, *Development and manufacturing an automated lubrication machine test for nano grease,* Journal of Materials Research and Technology, vol. 9, iss. 2, pp. 2054–2062, 2020, doi: 10.1016/j.jmrt.2019.12.038

[29] T. Li, B. Pan, C. Wang, S. Zhang, and S. Huang, *Effect of eco-friendly carbon microspheres on the tribological behavior of lithium lubricating grease, UPB Sci. Bull. Ser. B*, vol. 81, pp. 57–68, 2019.

[30] S. Ma, S. Zheng, D. Cao, H. Guo, *Anti-wear and friction performance of ZrO2 nanoparticles as lubricant additive,* Particuology, vol. 8, iss. 5, pp. 468–472, 2010, doi: 10.1016/j.partic.2009.06.007

[31] W.K. Shafi, M.S. Charoo, *Effect of temperature, concentration and aggregation on the rheological behavior of zro2–avocado oil nanolubricant,* Tribology in Industry, vol. 42, no. 3, p. 407–418, 2020, doi: 10.24874/ti.864.03.20.06

[32] W.K. Shafi, M.S. Charoo, *Rheological properties of hazelnut oil mixed with zirconium-dioxide nanoparticles*, Materials Today: Proceedings, vol. 26, pp. 745–749, 2020, doi: 10.1016/j.matpr.2020.01.019

[33] A. Rylski, K. Siczek, *The effect of addition of nanoparticles, especially ZrO2-based, on tribological behavior of lubricants,* Lubricants, vol. 8, iss. 3, pp. 1–25, 2020, doi: 10.3390/lubricants8030023

[34] X.T. Xia, Y.P. Zhang, Y.Z. Zhang, S.C. Chen, *Influence of ZrO2 nanoparticle as additive on tribological property of Lithium grease,* Applied Mechanics and Materials, 2010, vol. 26, pp. 83–87, doi: 10.4028/www.scientific.net/AMM.26-28.83

[35] S.F. Wang, J. Zhang, D. W. Luo, F. Gu, D.Y. Tang, Z.L. Dong, G.E.B. Tan, W.X. Que, T.S. Zhang, S. Li, L.B. Kong, *Transparent ceramics: Processing, materials and applications,* Progress in solid state chemistry, vol. 41, iss. 1–2, pp. 20–54, 2013, doi: 10.1016/j.progsolidstchem.2012.12.002

[36] D.S. Saini, S.P.S. Matharu, *Synthesis of Zirconium di-oxide powder from micro size to nano-size using high energy ball mill, AIP* Conference Proceedings, 2020, vol. 2273, iss. 1, doi: 10.1063/5.0024420

[37] R.H. Nielsen, J.H. Schlewitz, H. Nielsen, U. by Staff, *Zirconium and zirconium compounds,* Kirk-Othmer Encyclopedia of Chemical Technology, Wiley Online Library, 2000, doi: 10.1002/0471238961.26091803.a01.pub2

[38] P. Sahoo, *Engineering tribology*, PHI Learning Pvt. Ltd., 2005.

[39] ASTM D4172-94, *Standard Test Method for Wear Preventive Characteristics of Lubricating Fluid (Four- Ball Method)*, 1999.

[40] I. Asiltürk, H. Akkuş, *Determining the effect of cutting parameters on surface roughness in hard turning using the Taguchi method,* Measurement, vol. 44, iss. 9, pp. 1697–1704, 2011, doi: 10.1016/j.measurement.2011.07.003

[41] R.S. Parihar, R.K. Sahu, S.G. Setti, *Adhesive wear performance of self-lubricating functionally graded cemented tungsten carbide prepared by spark plasma sintering,* International Journal of Refractory Metals and Hard Materials, vol. 104, 2022, doi: 10.1016/j.ijrmhm.2022.105788

[42] T. Kıvak, *Optimization of surface roughness and flank wear using the Taguchi method in milling of Hadfield steel with PVD and CVD coated inserts*, Measurement, vol. 50, pp. 19–28, 2014, doi: 10.1016/j.measurement.2013.12.017

[43] M.K. Sahu, R. K. Sahu, *Investigation of Mechanical Properties and Optimization of Forming Parameters of Al7075-B4C-Fly Ash Hybrid Aluminium Matrix Composite,* Arabian Journal for Science and Engineering, vol. 47. pp. 8161–8176, 2022, doi: 10.1007/s13369-021-06117-1

[44] M.K. Sahu, R.K. Sahu, *Experimental investigation, modeling, and optimization of wear parameters of B4C and fly-ash reinforced aluminum hybrid composite*, Frontiers in Physics, vol. 8, pp. 1–14, 2020, doi: 10.3389/fphy.2020.00219

[45] N.F. Azman. S. Samion, *Dispersion stability and lubrication mechanism of nanolubricants: a review,* International journal of precision engineering and manufacturing-green technology, vol. 6, iss. 2, pp. 393–414, 2019, doi: 10.1007/s40684-019-00080-x

[46] B. Jaleh, S. Sodagar, A. Momeni, A. Jabbari, *Nanodiamond particles/PVDF nanocomposite flexible films: thermal, mechanical and physical properties,* Materials research express, vol. 3, no. 8, 2016, doi: 10.1088/2053-1591/3/8/085028

[47] S. Jana, S. Garain, S. Sen, D. Mandal, *The influence of hydrogen bonding on the dielectric constant and the piezoelectric energy harvesting performance of hydrated metal salt mediated PVDF films,* Physical Chemistry Chemical Physics, vol. 17, iss. 26, pp. 17429–17436, 2015, doi: 10.1039/C5CP01820J

[48] R.B. Rastogi, J.L. Maurya, V. Jaiswal, *Zero SAPS and ash free antiwear additives: Schiff bases of salicylaldehyde with 1, 2-phenylenediamine, 1, 4-phenylenediamine, and 4, 4′-diaminodiphenylenemethane and their synergistic interactions with borate ester,* Tribology transactions, vol. 56, iss. 4, pp. 592–606, 2013, doi: 10.1080/10402004.2012.748115

[49] R.N. Gupta, A.P. Harsha, *Antiwear and extreme pressure performance of castor oil with nano-additives,* Proceedings of the Institution of Mechanical Engineers, Part J: Journal of Engineering Tribology, vol. 232, iss. 9, pp. 1055–1067, 2018, doi: 10.1177/1350650117739159

[50] Z.S. Hu, J.X. Dong, G.X. Chen, *Study on antiwear and reducing friction additive of nanometer ferric oxide,* Tribology International, vol. 31, iss. 7, pp. 355–360, 1998, doi: 10.1016/S0301-679X(98)00042-5

[51] M. Merschdorf, W. Pfeiffer, A. Thon, S. Voll, G. Gerber, *Photoemission from multiply excited surface plasmons in Ag nanoparticles*, Applied Physics A, vol. 71, iss. 5, pp. 547–552, 2000, doi: 10.1007/s003390000712

[52] W. Li, S. Zheng, B. Cao, S. Ma, *Friction and wear properties of ZrO2/SiO2 composite nanoparticles,* Journal Nanoparticle Research, vol. 13, iss. 5, pp. 2129–2137, 2011, doi: 10.1007/s11051-010-9970-x

[53] M.R. Lovell, M.A. Kabir, P.L. Menezes, C.F. Higgs III, *Influence of boric acid additive size on green lubricant performance,* Philosophical Transactions of the Royal Society A: Mathematical, Physical and Engineering Sciences, vol. 368, no. 1929, pp. 4851–4868, 2010, doi: 10.1098/rsta.2010.0183

[54] R. Wäsche, M. Hartelt, V.-D. Hodoroaba, *Analysis of nanoscale wear particles from lubricated steel–steel contacts*, Tribology Letters, vol. 58, iss. 3, pp. 1–10, 2015, doi: 10.1007/s11249-015-0534-1

[55] R.N. Gupta, A.P. Harsha, *Synthesis, Characterization, and Tribological Studies of Calcium – Copper – Titanate Nanoparticles as a Biolubricant Additive,* Journal of Tribology, vol. 139, iss. 2, pp. 1–11, 2017, doi: 10.1115/1.4033714

[56] K. Lee, Y. Hwang, S. Cheong, Y. Choi, L. Kwon, J. Lee, S.H. Kim, *Understanding the role of nanoparticles in nano-oil lubrication,* Tribology Letters, vol. 35, iss. 2, pp. 127–131, 2009, doi: 10.1007/s11249-009-9441-7

[57] H. Ghaednia, R.L. Jackson, *The Effect of Nanoparticles on the Real Area of Contact , Friction , and Wear,* Journal of Tribology, vol. 135, iss. 4, pp. 1–10, 2013, doi: 10.1115/1.4024297

[58] M.H. Cetin, B. Ozcelik, E. Kuram, E. Demirbas, *Evaluation of vegetable based cutting fluids with extreme pressure and cutting parameters in turning of AISI 304L by Taguchi method,* Journal of Cleaner Production, vol. 19, iss. 17–18, pp. 2049–2056, 2011, doi: 10.1016/j.jclepro.2011.07.013

NOMENCLATURE

∅	Volume Fraction/ Concentration
μ	Friction coefficient
W	Applied load (N)
T	Friction torque (N.m)
R	Distance from the center (mm)
d_p	Diameter of Nano-particle (nm)
ρ_{np}	Density of nano-particles
ρ_{bf}	Density of Base fluid
w_{np}	Weight of nano-particle (g)
w_{bf}	Weight of base fluid (g)
Y_i	Outcome of the i^{th} Experiment
n	Total number of observation (in this case n=3)
FESEM	Field emission scanning electron microscopy
CoF	Coefficient of Friction
EDX	Energy Dispersive X-ray
ASTM	American Society for Testing and Materials
WV	Wear Variation
MWV	Mean Wear Volume
S/N	Signal-to-noise ratio
MGO	Multigrade oil
SAE	Society of Automotive Engineering
FTIR	Fourier-transform infrared spectroscopy
RPM	Revolution per Minutes
R^2	Coefficient of determination
DOE	Design of Experiment
APS	Average Particle Size
WSD	Wear Scar Diameter
np	nano-particle
nf	nano-fluid
bf	base-fluid